Journal of Sound and Vibration (1999) **220**(5), 905–920
Article No. jsvi.1998.1977, available online at http://www.idealibrary.com.on IDEAL

PREDICTING THE ABSORPTION OF OPEN WEAVE TEXTILES AND MICRO-PERFORATED MEMBRANES BACKED BY AN AIR SPACE

J. KANG† AND H. V. FUCHS

Fraunhofer-Institut für Bauphysik (IBP), Nobelstr. 12, D-70569 Stuttgart, Germany

(*Received* 28 *April* 1997, *and in final form* 25 *September* 1998)

Although theories for both membrane absorbers and micro-perforated plate absorbers have been well developed, it appears that no theory has been given for their combination, such as a glass-fibre textile or a micro-perforated membrane mounted over an airtight cavity. This paper presents a theoretical method for predicting the absorption of such a structure. The basic idea of the theory is to regard an open weave textile or a micro-perforated membrane as a parallel connection of the membrane and apertures. The predictions for both normal and random incidence have shown very good agreement with measurements. It has also been demonstrated that the absorption performance of such structures can be very high. Typically, with appropriate parameters the absorption coefficient of a glass-fibre textile or a micro-perforated membrane mounted at 100 mm from a rigid wall can exceed 0·4 over 3–4 octaves. With two layers of the material over the same total air space of 100 mm this range can extend to 4–5 octaves.

1. INTRODUCTION

Theories for both the membrane absorber [1, 2], namely a limp lightweight membrane backed by an air space, and the micro-perforated absorber [3, 4], namely a cavity backed plate with low aperture ratio but many apertures of sub-millimetre size, have been well developed. However, it appears that no theory has been given for their combination, such as a glass-fibre textile or a micro-perforated membrane mounted over an airtight cavity. Measurements have shown that such a structure could act as a good absorber [5–7]. This absorber would have notable advantages in practice since it is lightweight, inexpensive, and due to the absence of loose fibrous material, less of a health concern than commonly used fibrous absorptive materials. In this paper, a theoretical method for predicting the absorption of this structure is described, and the predictions are compared with measurements. A series of parameter studies is also presented.

†Corresponding author. Current address: The Martin Centre, University of Cambridge, 6 Chaucer Road, Cambridge CB2 2EB, England.

0022–460X/99/100905 + 16 $30.00/0

2. THEORY

2.1. SINGLE LAYER

For an open weave textile or a micro-perforated membrane backed by an air space, since the resonance frequencies caused by the membrane and by the apertures can be in the same range, their simultaneous effects should be considered. The basic idea of the proposed theory is to regard an open weave textile or a micro-perforated membrane as a parallel connection of the membrane and apertures. In this way the effectiveness of one element relies on its relative impedance to the other. In other words, if the acoustic impedance of the apertures is much greater than that of the membrane, the absorption of the structure depends mainly on the characteristics of the membrane, and conversely, the apertures will play a dominant role if their acoustic impedance is much less than that of the membrane. In order to modify the absorption, the acoustic impedance of the structure can be adjusted by varying the appropriate parameters of the membrane and the apertures.

An open weave textile or a micro-perforated membrane backed by an air space makes a resonant system. The acoustic impedance of such a system can be obtained using the impedance type of electro-acoustic analogy. Basically, the resonant system contains the mass-resistance element in series with the cavity reactance of the air space. As mentioned above, the mass-resistance element consists of the membrane and the apertures being connected in parallel. In Figure 1 is shown the equivalent circuit of a single layer of open weave textile or micro-perforated membrane mounted at distance D (m) from a rigid wall, where R_M and M_M are the specific acoustic resistance and reactance of the membrane,

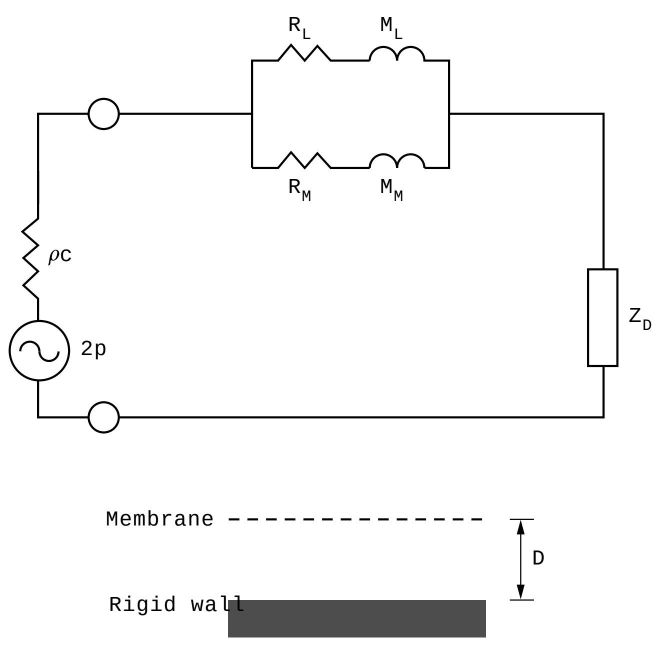

Figure 1. A structure with a single layer of open weave textile or micro-perforated membrane and the equivalent circuit of this structure.

and R_L and M_L are the specific acoustic resistance and reactance of the apertures. The sound wave impinging on the structure is equivalent to a source of sound pressure $2p$ as produced on the rigid wall (analogous to the open-circuit voltage) and internal resistance ρc as that of air [4].

From Figure 1 it can be seen that in order to obtain the acoustic impedance of the whole system, it is necessary to consider the impedance of each element. Consider first an unperforated membrane. For a tension-free membrane mounted at some distance from a rigid wall, the normal specific acoustic impedance of the membrane normalized by ρc can be calculated by

$$z_M = \frac{R_M + \mathrm{j}M_M}{\rho c} = r' + \mathrm{j}\omega m'' \tag{1}$$

where ρ is the density of air and c is the sound velocity in air. $\omega = 2\pi f$, f is the frequency (Hz). $m'' = m'/\rho c$, m' is the surface density of the membrane (kg/m^2). r' is the normalized specific acoustic resistance of the membrane, which depends mainly on mounting conditions.

Consider secondly the effect of the apertures alone. An aperture may be regarded as a short tube. The propagation of sound waves in narrow tubes was first discussed by Rayleigh [8], and a simplified version was given by Crandall [9] for very short tubes in comparison with wavelengths. For the equation of aerial motion inside the tube, by assuming sinusoidal functions of time and zero velocity on the tube wall, an exact solution for the acoustic impedance of the tube was derived. Because the calculation was rather complicated, Crandall proposed two approximate formulae for both small and large apertures that can be used for porous materials and conventional perforated plates respectively. Maa [3, 4], observing the discontinuity between the two cases, developed an approximate solution for apertures of sub-millimetre size, namely for micro-perforated plates. A micro-perforated plate backed by an air space can still be regarded as a mass–spring system. In comparison with conventional formulae for perforated plate absorbers, however, an outstanding feature of Maa's theory is that the acoustic resistance of the apertures, which becomes significant when the apertures are very small, is taken into account. Consequently, for micro-perforated absorbers it is not necessary to provide extra acoustic resistance using porous materials. According to Maa, for normal incidence, the normalized specific acoustic impedance of the apertures can be calculated by

$$z_L = \frac{R_L + \mathrm{j}M_L}{\rho c} = r + \mathrm{j}\omega m \tag{2}$$

with

$$r = \frac{g_1}{d^2}\frac{t}{p}K_r \tag{3}$$

$$m = 0{\cdot}294(10^{-3})\,\frac{t}{p}\,K_m \tag{4}$$

$$K_r = \sqrt{1 + \frac{x^2}{32}} + \frac{x\sqrt{2}}{8}\frac{d}{t} \tag{5}$$

$$K_m = 1 + \frac{1}{\sqrt{9 + \frac{x^2}{2}}} + 0{\cdot}85\,\frac{d}{t} \tag{6}$$

$$x = g_2 d\sqrt{f} \tag{7}$$

where t is the membrane thickness (mm), d is the aperture diameter (mm), p is the aperture ratio (aperture area/membrane area), and b is the distance between aperture centres (mm). g_1 and g_2 are constants. For a non-metallic material, $g_1 = 0{\cdot}147$ and $g_2 = 0{\cdot}316$. For a metallic material, $g_1 = 0{\cdot}335$ and $g_2 = 0{\cdot}21$. The above equations are used for circular apertures. For square apertures with a side l (mm), an approximation can be made by using the same aperture area [5], namely $d = 2l\sqrt{1/\pi}$. In equation (5) the second term is the end correction for resistance. Similarly, the last term in equation (6) is the end correction for mass reactance. It is noted that equations (3)–(7) are restricted to air under standard conditions of temperature and pressure.

The normal specific acoustic impedance of the air behind the membrane, again normalized by ρc, is

$$z_D = -\mathrm{j}\,\mathrm{ctg}\left(\frac{\omega D}{c}\right). \tag{8}$$

According to the equivalent circuit in Figure 1, the normalized normal specific acoustic impedance of the whole structure can be calculated by

$$z = \frac{z_M z_L}{z_M + z_L} + z_D = H_r + \mathrm{j}\left(H_m - \mathrm{ctg}\,\frac{\omega D}{c}\right) \tag{9}$$

with

$$H_r = \frac{H_a H_c + H_b H_d}{H_c^2 + H_d^2} \tag{10}$$

$$H_m = \frac{H_b H_c - H_a H_d}{H_c^2 + H_d^2} \tag{11}$$

$$H_a = rr' - \omega^2 mm'' \tag{12}$$

$$H_b = r'\omega m + r\omega m'' \tag{13}$$

$$H_c = r + r' \tag{14}$$

$$H_d = \omega(m + m''). \tag{15}$$

The absorption coefficient can then be calculated by the well-known formula:

$$\alpha = \frac{4\,\mathrm{Re}\,(z)}{[1+\mathrm{Re}\,(z)]^2+[\mathrm{Im}\,(z)]^2} = \frac{4H_r}{(1+H_r)^2+\left(H_m-\mathrm{ctg}\,\dfrac{\omega D}{c}\right)^2}. \tag{16}$$

The maximum absorption coefficient is

$$\alpha_{max} = \frac{4H}{(1+H_r)^2}. \tag{17}$$

As with other resonant absorbers, there are multiple resonance frequencies for the above structure, which can be calculated by using

$$H_m - \mathrm{ctg}\,\frac{\omega D}{c} = 0. \tag{18}$$

Between the multiple resonances there are zero points in absorption, which occur at the frequencies making $\mathrm{ctg}\,(\omega D/c)$ infinite.

2.2. OBLIQUE AND RANDOM INCIDENCE

The membrane itself and the apertures are locally reacting acoustic elements [2–4]. That is, the acoustic impedance is independent of the angle of incidence. Conversely, the impedance of the air space will change due to the change of the path difference between the incident and reflected waves. Overall, when the sound wave is incident under an angle θ to the normal, equation (9) becomes

$$z_\theta = H_r\cos\theta + \mathrm{j}\left(H_m\cos\theta - \frac{1}{\cos\theta}\,\mathrm{ctg}\,\frac{\omega D\cos\theta}{c}\right). \tag{19}$$

Using equation (17) it can be demonstrated that in comparison with normal incidence the maximum absorption coefficient for oblique incidence is less if $H_r \leqslant 1$, and can be greater when $H_r > 1$. It can also be proved that for oblique incidence the absorption range will shift to higher frequencies [3].

In a diffuse sound field, the angle-averaged absorption coefficient can be obtained from

$$\alpha_0 = 2\int_0^{\pi/2} \alpha_\theta \sin\theta\cos\theta\,\mathrm{d}\theta. \tag{20}$$

Clearly the zero points in absorption between the multiple resonances will disappear due to the angle average. In other words, the troughs in the absorption curve between the multiple resonances will be less deep in comparison with those under normal incidence condition. This is especially useful for wideband absorbers like open weave textiles or micro-perforated membranes. Similar to oblique incidence, in a diffuse field the resonance frequencies will be higher than those for normal incidence.

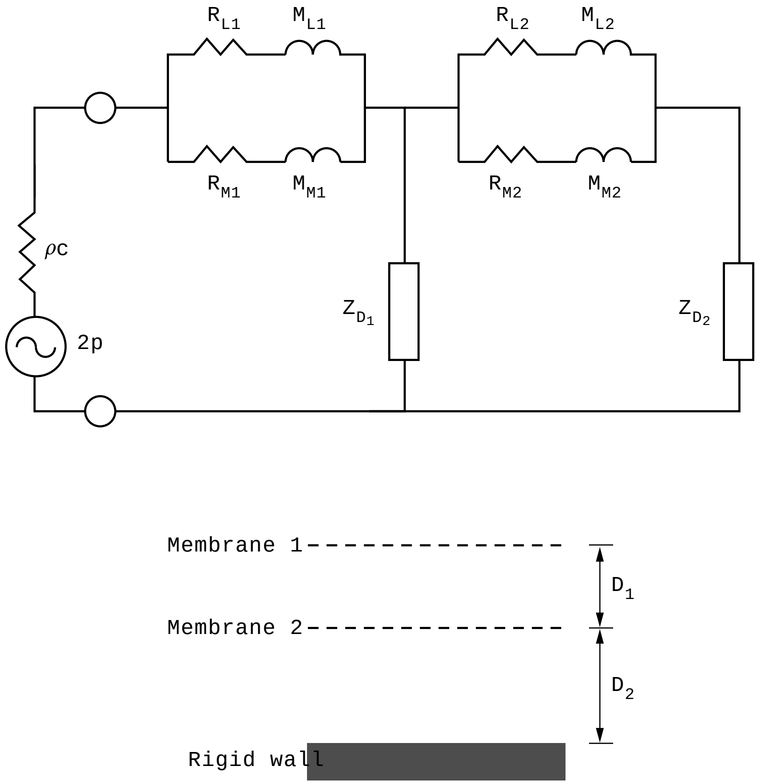

Figure 2. A structure with two layers of open weave textile or micro-perforated membrane and the equivalent circuit of this structure.

2.3. DOUBLE LAYER

To broaden the frequency range of absorption, it is effective to use more layers of membrane. In Figure 2 is shown a structure with two layers of open weave textile or micro-perforated membrane and the equivalent circuit of this structure, where D_1 (m) is the distance between the two layers and D_2 (m) is the distance from the inner layer to the rigid wall. In correspondence with the double resonator formed by the structure, the equivalent circuit has a second resonance circuit added parallel with Z_{D1}. According to the equivalent circuit in Figure 2, the normalized normal specific acoustic impedance of the whole structure can be calculated by

$$z = H_{r1} + \mathrm{j}\left(H_{m1} - \mathrm{ctg}\,\frac{\omega D_1}{c}\right) + \frac{\mathrm{ctg}^2\,\dfrac{\omega D_1}{c}}{H_{r2} + \mathrm{j}\left(H_{m2} - \mathrm{ctg}\,\dfrac{\omega D_1}{c} - \mathrm{ctg}\,\dfrac{\omega D_2}{c}\right)}$$

$$= H_{r1} + \frac{H_C H_{r2}}{H_B^2 + H_{r2}^2} + \mathrm{j}\left(H_A - \frac{H_B H_C}{H_B^2 + H_{r2}^2}\right) \tag{21}$$

with

$$H_A = H_{m1} - \mathrm{ctg}\,\frac{\omega D_1}{c} \tag{22}$$

$$H_B = H_{m2} - \mathrm{ctg}\,\frac{\omega D_1}{c} - \mathrm{ctg}\,\frac{\omega D_2}{c} \tag{23}$$

$$H_C = \mathrm{ctg}^2\left(\frac{\omega D_1}{c}\right) \tag{24}$$

where H_{r1} and H_{m1} are calculated using the parameters of the outer membrane, and H_{r2} and H_{m2} are in correspondence with the inner membrane.

When only considering the effect of apertures, it has been theoretically demonstrated by Maa [3] that in comparison with a single layer micro-perforated plate with D_1, when there are two micro-perforated layers with $D_1 + D_2$, the low frequency range of absorption can be exteneded approximately from f_l to $f_l[D_1/(D_1 + D_2)]$. By using equation (21) it can be proved that this is also true when the effect of the membrane is taken into account. At relatively high frequencies, namely higher than the resonance frequency of the inner layer, by using the first expression of equation (21) it can be proved that the acoustic reactance of two layers is approximately the same as that of the outer layer alone with D_1. This means that using an additional layer may not increase the high frequency range of absorption. As for the acoustic resistance, from the second expression of equation (21) it is seen that using an extra layer can increase the real component of the acoustic impedance.

For a wave impinging on the structure at an angle θ to the normal, in equations (21)–(24) H_{r1}, H_{r2}, H_{m1}, H_{m2}, D_1 and D_2 should be multiplied by $\cos\theta$. Consequently, the diffuse field absorption coefficient can be calculated using equation (20).

A C-program has been developed for the above equations. If a language, such as Matlab, which supports complex variables, is used, the programming can be simplified considerably.

3. EFFECT OF PARAMETER VARIATIONS

Since the relationships between the parameters above are rather complicated, it is difficult to examine analytically the effects of those parameters on the absorption characteristics of a structure. In this section, therefore, a series of numerical studies is carried out.

3.1. SINGLE LAYER

From equations (1) to (18) it is seen that the absorption characteristics of an open weave textile or micro-perforated membrane are dependent on p, l, b, m' and t. The effects of these parameters are analysed below, based on a series of theoretical calculations in accordance with an actual textile (see section 4.1). For the sake of convenience, the calculation is limited to a single layer with $D = 100$ mm.

The effects of p, l and b, namely the aperture ratio, size and spacing, are shown in Figure 3. In the calculation, $m' = 0{\cdot}19$ kg/m^2 and $t = 0{\cdot}17$ mm. From Figure 3 it is important to note that for an open weave textile or micro-perforated membrane, such as with $l = 0{\cdot}06$ mm and $b = 0{\cdot}66$ mm ($p = 0{\cdot}83\%$), the frequency range of absorption increases in comparison with an unperforated membrane. For a given aperture ratio, the aperture size also affects the absorption characteristics. From equations (3), (5) and (7) it can be demonstrated that for a constant p, with the increase of d or l, r becomes less, and consequently, the absorption coefficient of the whole structure may be decreased. For example, with $p = 0{\cdot}83\%$ but $l = 0{\cdot}3$ mm and $b = 3{\cdot}3$ mm, the absorption coefficient is lower, and the resonance frequency is slightly higher than that with $l = 0{\cdot}06$ mm and $b = 0{\cdot}66$ mm. If the aperture ratio is too high, for instance, with $p = 7{\cdot}43\%$ ($l = 0{\cdot}18$ mm and $b = 0{\cdot}66$ mm) or even $p = 20{\cdot}65\%$ ($l = 0{\cdot}3$ mm and $b = 0{\cdot}66$ mm), the absorption coefficient can be significantly decreased. Clearly this is because the acoustic resistance of the structure becomes less with the increase of aperture ratio.

The effect of m', namely the membrane surface density, is demonstrated in Figure 4. In the calculation, $t = 0{\cdot}17$ mm, $l = 0{\cdot}06$ mm, and $b = 0{\cdot}66$ mm ($p = 0{\cdot}83\%$). As expected, with increasing surface density, the resonance frequency becomes lower. In Figure 4 it is seen that with a range of $m' = 0{\cdot}19$–$1{\cdot}9$ kg/m^2, the resonance frequency varies from 400 to 160 Hz.

The effect of t, namely the membrane thickness, is shown in Figure 5. In the calculation, $m' = 0{\cdot}19$ kg/m^2, $l = 0{\cdot}06$ mm and $b = 0{\cdot}66$ mm ($p = 0{\cdot}83\%$). From Figure 5 it is seen that with the increase of t, the resonance frequency becomes lower. This is expected. However, it is noted that this variation is not significant

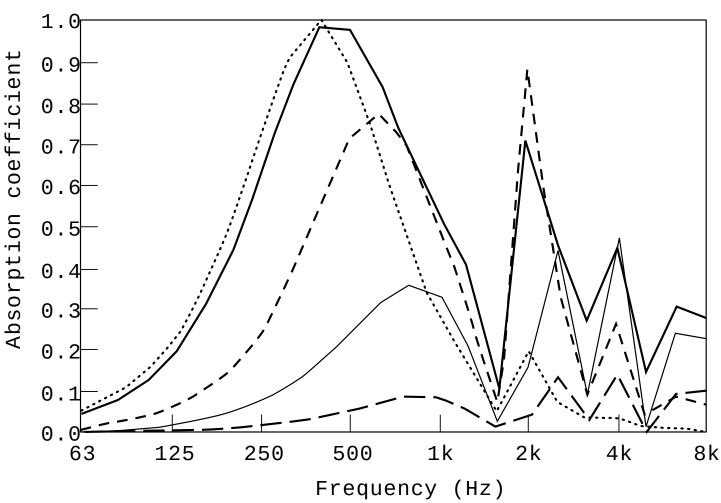

Figure 3. The calculated normal incidence absorption coefficient of a structure with $D = 100$ mm, $m' = 0{\cdot}19$ kg/m^2 and $t = 0{\cdot}17$ mm. . . . . , unperforated; ——, $l = 0{\cdot}06$ mm and $b = 0{\cdot}66$ mm ($p = 0{\cdot}83\%$); - - - - , $l = 0{\cdot}3$ mm and $b = 3{\cdot}3$ mm ($p = 0{\cdot}83\%$); ——, $l = 0{\cdot}18$ mm and $b = 0{\cdot}66$ mm ($p = 7{\cdot}43\%$); — — —, $l = 0{\cdot}3$ mm and $b = 0{\cdot}66$ mm ($p = 20{\cdot}65\%$). Single-frequency values at one-third octave intervals.

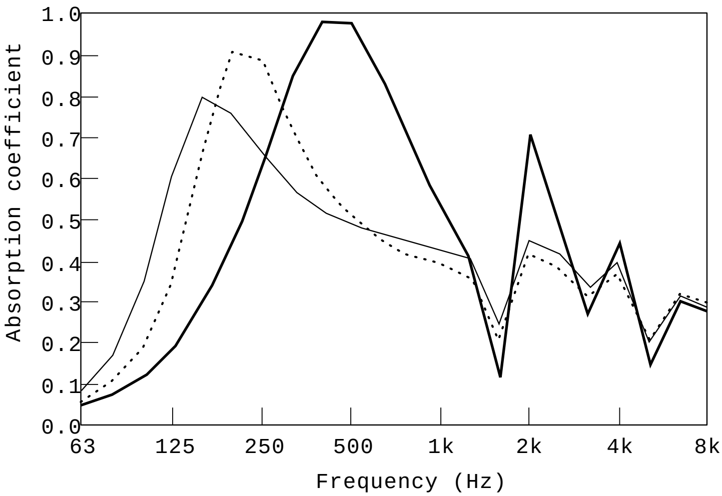

Figure 4. The calculated normal incidence absorption coefficient of a structure with $D = 100$ mm, $t = 0{\cdot}17$ mm, $l = 0{\cdot}06$ mm and $b = 0{\cdot}66$ mm ($p = 0{\cdot}83\%$). ——, $m' = 1{\cdot}9$ kg/m^2; . . . . , $m' = 0{\cdot}95$ kg/m^2; ——, $m' = 0{\cdot}19$ kg/m^2. Single-frequency values at one-third octave intervals.

over the extensive range of membrane thickness considered. For example, when t varies from 0·05 to 1·7 mm, the variation in resonance frequency is only within a one-third octave band.

3.2. DOUBLE LAYER

For two layer structures, the effects of D_1 and D_2 are theoretically analysed below in accordance with a micro-perforated membrane of $m' = 0{\cdot}14$ kg/m^2, $t = 0{\cdot}11$ mm, $d = 0{\cdot}2$ mm and $b = 2$ mm ($p = 0{\cdot}79\%$), which is also an actual material (see section 4.2).

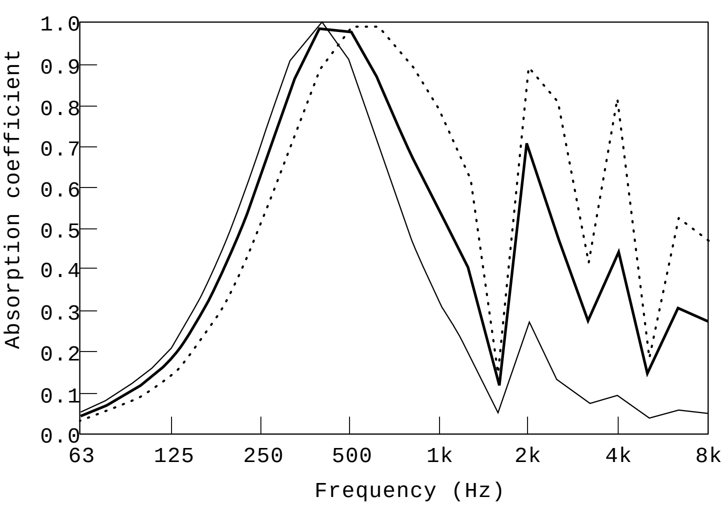

Figure 5. The calculated normal incidence absorption coefficient of a structure with $D = 100$ mm, $m' = 0{\cdot}19$ kg/m^2, $l = 0{\cdot}06$ mm and $b = 0{\cdot}66$ mm ($p = 0{\cdot}83\%$). ——, $t = 1{\cdot}7$ mm; ——, $t = 0{\cdot}17$ mm; . . . . . , $t = 0{\cdot}05$ mm. Single-frequency values at one-third octave intervals.

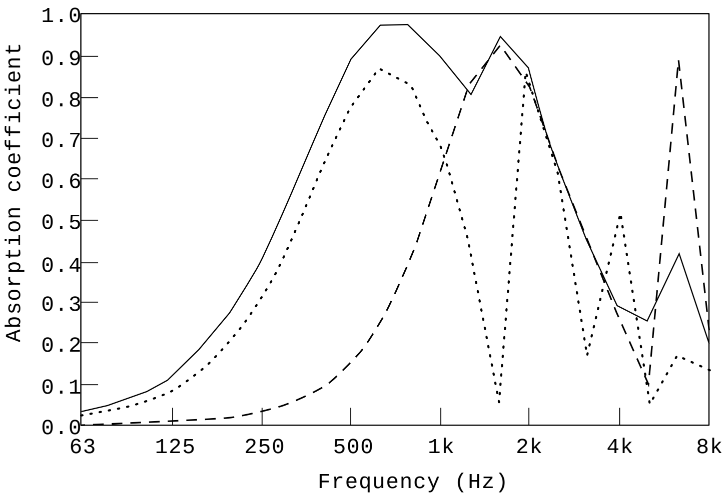

Figure 6. The comparison of calculated normal incidence absorption coefficient between one and two layers of a micro-perforated membrane with $m' = 0{\cdot}14$ kg/m^2, $t = 0{\cdot}11$ mm, $d = 0{\cdot}2$ mm and $b = 2$ mm ($p = 0{\cdot}79\%$). - - - , $D = 30$ mm; . . . . , $D = 100$ mm; ——, $D_1 = 30$ mm and $D_2 = 70$ mm. Single-frequency values at one-third octave intervals.

The calculated absorption coefficients with $D = 30$ mm, 100 mm and $D_1 + D_2 = 30 + 70$ mm are shown in Figure 6. As expected, in comparison with $D = 30$ mm, with $D_1 + D_2 = 30 + 70$ mm the high frequency range of absorption is almost the same, but the low frequency range of absorption is significantly extended. In comparison with $D = 100$ mm, with $D_1 + D_2 = 30 + 70$ mm the absorption is extended in both high and low frequency directions, and also, the absorption coefficient is increased. An important reason for this increase is that with two layers the acoustic resistance is increased, as indicated previously.

When D_2 is significantly greater than D_1, there might be a deep trough in the absorption curve between the resonances of the two layers. This trough, however, could be more or less diminished by the multiple resonances of the inner layer. For random incidence the trough can be even less. Such an example is given in Figure 7, with $D_1 + D_2 = 20 + 280$ mm.

4. MEASUREMENTS

To validate the theory, a series of measurements was carried out in an impedance tube as well as in a reverberation room. The comparisons between calculation and measurement are presented below.

4.1. IMPEDANCE TUBE

The cross-section of the impedance tube was 200 mm by 200 mm. A program corresponding to a single microphone fast Fourier transform method was used for measuring the impedance and absorption coefficient [10, 11]. The measured absorption coefficients were one-twelfth octave band averages, presented in this paper at one-third octave intervals. Two kinds of glass-fibre textiles were measured, one with $m' = 0{\cdot}19$ kg/m^2, $t = 0{\cdot}17$ mm, $l = 0{\cdot}06$ mm and $b = 0{\cdot}66$ mm

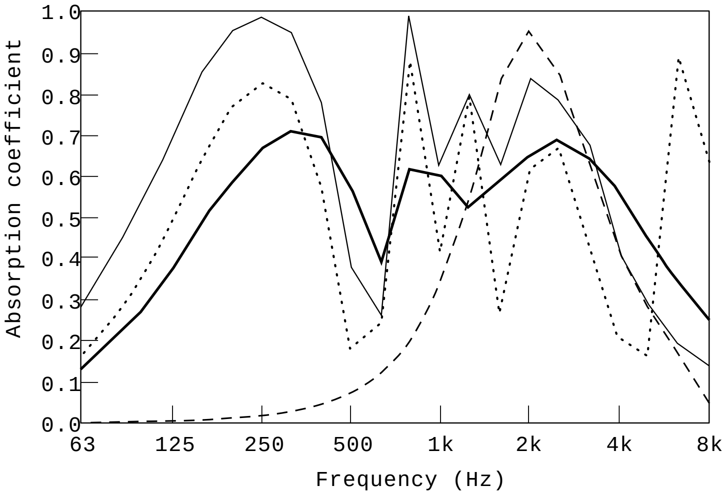

Figure 7. The comparison of calculated absorption coefficient between one and two layers of a micro-perforated membrane with $m' = 0{\cdot}14$ kg/m^2, $t = 0{\cdot}11$ mm, $d = 0{\cdot}2$ mm and $b = 2$ mm ($p = 0{\cdot}79\%$). (1) Single layer, normal incidence: - - - , $D = 20$ mm; . . . . , $D = 300$ mm. (2) Double layer, $D_1 = 20$ mm and $D_2 = 280$ mm: ——, normal incidence; ——, random incidence. single-frequency values at one-third octave intervals.

($p = 0{\cdot}83\%$), and the other with $m' = 0{\cdot}13$ kg/m^2, $t = 0{\cdot}13$ mm, $l = 0{\cdot}18$ mm and $b = 0{\cdot}83$ mm ($p = 4{\cdot}7\%$). The former was experimentally developed for use as a standalone absorber [5, 6], and the latter was an ordinary glass-fibre textile, frequently used as a cover for porous absorbers. In the following, for the sake of convenience, the two materials are called textiles A and B, respectively. In the measurements the textiles were firmly stuck on a frame of 200 mm by 200 mm, which was the same as the cross-section of the impedance tube.

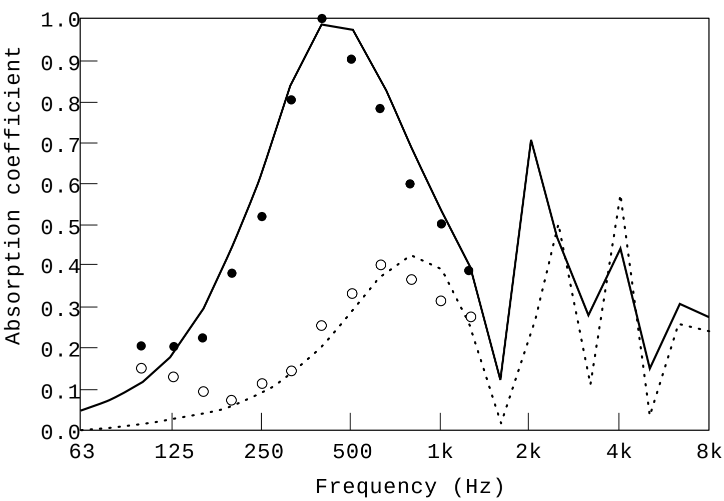

Figure 8. The comparison between calculated (single-frequency) and measured (one-twelfth octave band average) normal incidence absorption coefficients for textile A (——, calculation; ●, measurement) and textile B (. . . . , calculation; ○, measurement). $D = 100$ mm.

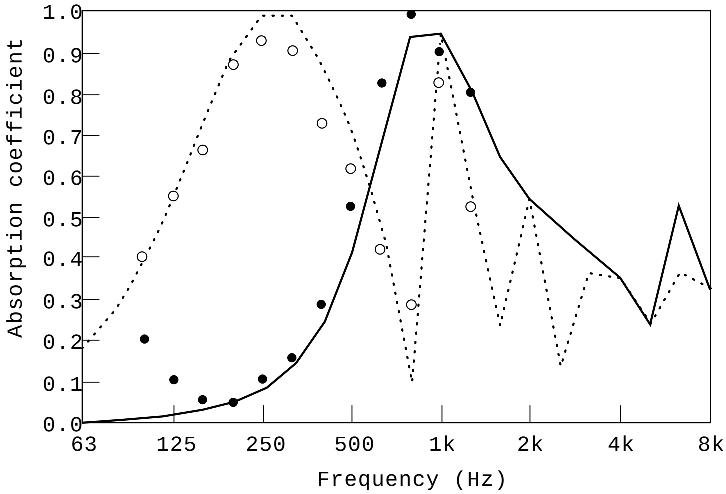

Figure 9. The comparison between calculated (single-frequency) and measured (one-twelfth octave band average) normal incidence absorption coefficients for textile A with $D = 30$ mm (——, calculation; ●, measurement) and $D = 200$ mm (. . . , calculation; ○, measurement).

In Figure 8 is shown the comparison between calculated and measured absorption coefficients for the above two textiles, with $D = 100$ mm. It can be seen that the agreement between calculation and measurement is impressive and generally within $\pm 0{\cdot}1$ accuracy. In the calculation, r' is around 1, which has been experimentally proved to be appropriate to the mounting condition [12].

It is important to note that the absorption coefficient of textile A is significantly higher than that of textile B. With textile A, the absorption coefficient exceeds 0·4 in the range 200–1·25 kHz, whereas with textile B this range is only about 630–1 kHz. Clearly this is attributable to differences in the aperture ratio, spacing and size between the two textiles.

With $D = 30$ mm and 200 mm, the comparisons between calculated and measured absorption coefficients for textiles A and B are shown in Figures 9 and 10, respectively. The agreement between calculation and measurement is also very good. For textile A, with $D = 30$–200 mm, a considerable frequency range of absorption can be obtained, i.e., $\alpha > 0{\cdot}4$ from 100 Hz to 3·15 kHz. In the measurements with $D = 200$ mm, it is interesting to note that multiple resonances can be clearly seen for both textiles A and B. This is in correspondence with the theory.

For double layer textiles, comparisons between calculation and measurement were also made, with $D_1 = 30$ mm and $D_2 = 70$ mm, for both textiles A and B. The comparisons are shown in Figure 11. It is seen that the agreement between calculation and measurement is still very good. As expected, with two layers the frequency range of absorption is much wider than that of a single layer with an air space of 100 mm, namely $D_1 + D_2$. For two layers of textile A, the absorption coefficient exceeds 0·4 from 160 Hz to 3·15 kHz. For two layers of textile B, the absorption coefficient exceeds 0·4 from 500 Hz to 4 kHz, which is a significantly broader range than that measured for a single layer (i.e., 630–1 k Hz).

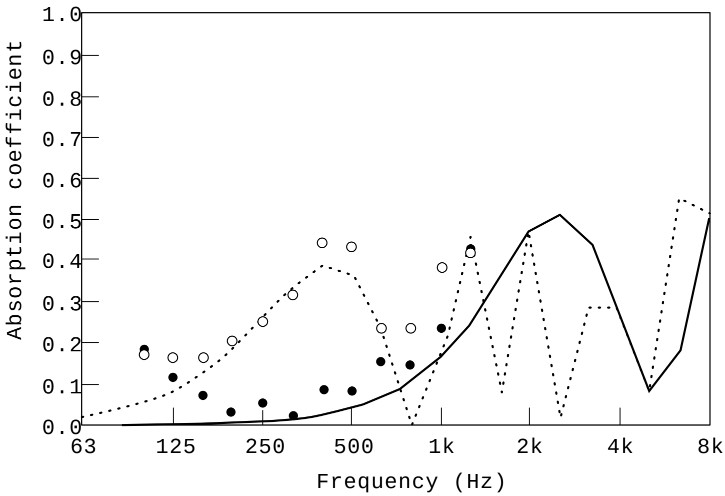

Figure 10. The comparison between calculated (single-frequency) and measured (one-twelfth octave band average) normal incidence absorption coefficients for textile B with $D = 30$ mm (——, calculation; ●, measurement) and $D = 200$ mm (. . . , calculation; ○, measurement).

4.2. REVERBERATION ROOM

In the reverberation room the measured frequency range was up to 5 kHz, which was much higher than that in the impedance tube. This is useful for further verifying the multiple resonances in absorption at relatively high frequencies, as shown in Figures 3–11. A micro-perforated plastic membrane of $m' = 0{\cdot}14$ kg/m^2, $t = 0{\cdot}11$ mm, $d = 0{\cdot}2$ mm and $b = 2$ mm ($p = 0{\cdot}79\%$) was measured [7].

The comparisons between calculated and measured absorption coefficients of a single layer of the membrane with $D = 100$ mm and 30 mm are shown in Figures

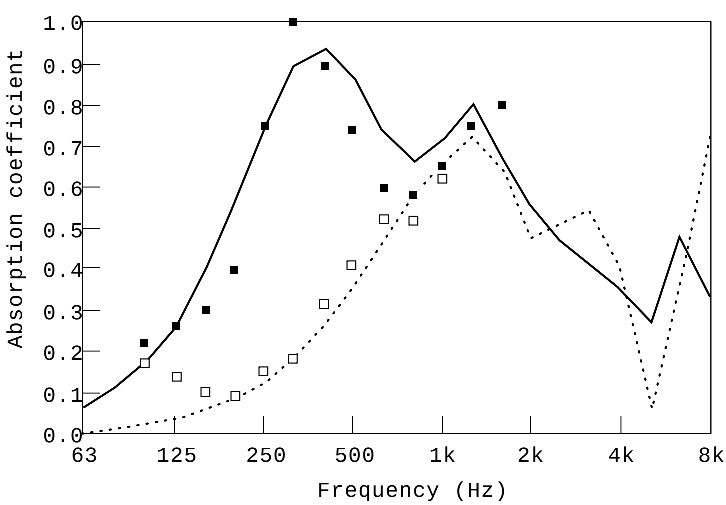

Figure 11. The comparison between calculated (single-frequency) and measured (one-twelfth octave band average) normal incidence absorption coefficients for two layers of textiles with $D_1 = 30$ mm and $D_2 = 70$ mm. (1) Textile A: ——, calculation; ■, measurement. (2) Textile B: . . . . , calculation; □, measurement.

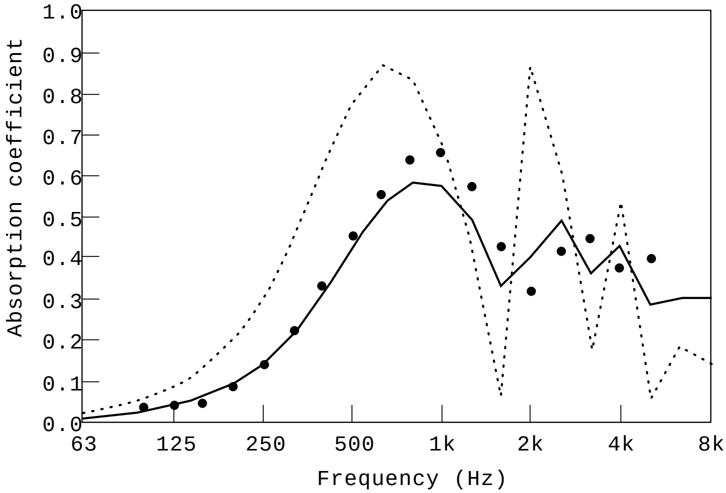

Figure 12. The calculated (single-frequency) and measured (one-third octave band average) diffuse field absorption coefficients (——, calculation; ●, measurement) and calculated (single-frequency) normal incidence absorption coefficient (. . . .) for the micro-perforated membrane with $D = 100$ mm.

12 and 13, respectively. The agreement between calculation and measurement is very good and generally within $\pm 0{\cdot}1$ accuracy. It is important to note that multiple resonances can be clearly seen in the measurement with $D = 100$ mm.

Comparisons between calculated and measured diffuse field absorption coefficients were also made for two layers of the micro-perforated membrane. The comparison with $D_1 = 30$ mm and $D_2 = 100$ mm is shown in Figure 14. Again, the agreement is very good. As with the results for normal incidence, the diffuse field

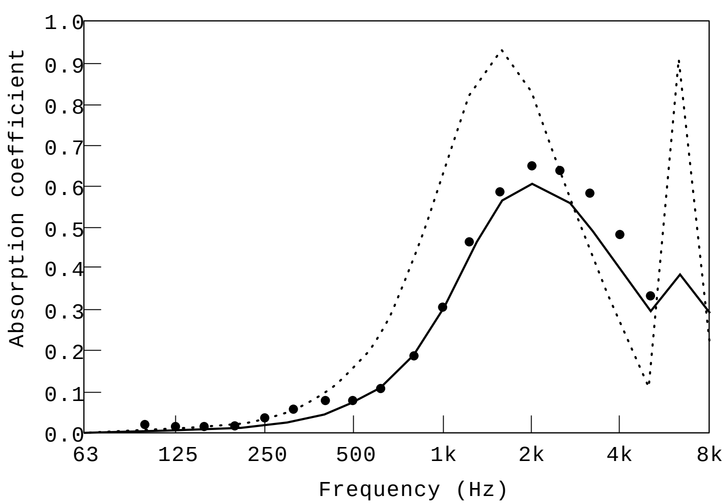

Figure 13. The calculated (single-frequency) and measured (one-third octave band average) diffuse field absorption coefficients (——, calculation; ●, measurement) and calculated (single-frequency) normal incidence absorption coefficient (. . . .) for the micro-perforated membrane with $D = 30$ mm.

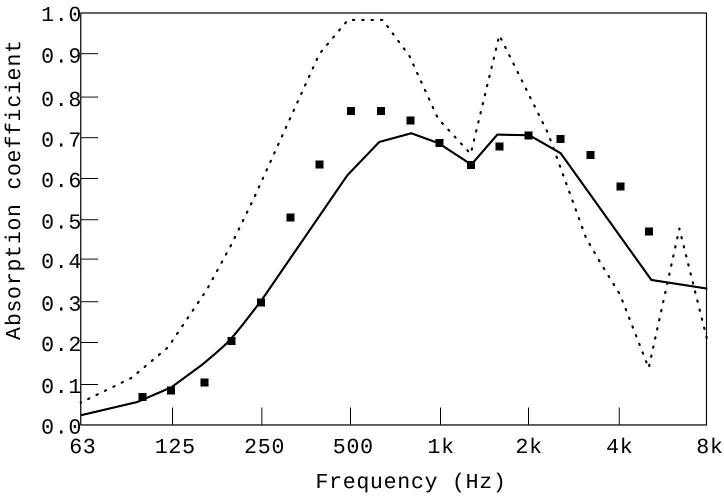

Figure 14. The calculated (single-frequency) and measured (one-third octave band average) diffuse field absorption coefficients (——, calculation; ■, measurement) and calculated (single-frequency) normal incidence absorption coefficient (. . . .) for two layers of the micro-perforated membrane with $D_1 = 30$ mm and $D_2 = 100$ mm.

absorption can also be considerably increased by using double layer membranes. From Figure 14 it can be seen that the diffuse field absorption coefficient exceeds 0·4 from 315 Hz to 5 kHz, which is encouraging.

In Figures 12, 13 and 14 comparisons between normal and diffuse field absorption coefficients are also made. As expected, in comparison with normal incidence, in a diffuse field the angle-averaged absorption coefficient is generally less, the resonances shift to higher frequencies, and the troughs in the absorption curve between multiple resonances are less deep.

5. CONCLUSIONS

A theoretical method has been developed for predicting the absorption of open weave textiles and micro-perforated membranes backed by an air space. The predictions for two kinds of glass-fibre textiles and a micro-perforated plastic membrane have shown very good agreement with measurements. The measurements were made in an impedance tube as well as in a reverberation room.

The absorption performance of the above structures can be very high. Typically, with appropriate parameters the absorption coefficient of a glass-fibre textile or a micro-perforated membrane mounted at 100 mm from a rigid wall can exceed 0·4 over 3–4 octaves. With two layers of the material over the same total air space of 100 mm this range can extend to 4–5 octaves.

ACKNOWLEDGMENTS

The first author would like to acknowledge the Alexander von Humboldt Foundation and the Lloyd Foundation for their financial supports.

REFERENCES

1. L. Cremer and H. Müller 1978 *Die Wissenschaftlichen Grundlagen der Raumakustik*. Stuttgart: Hirzel.
2. K. U. Ingard 1994 *Notes on Sound Absorption Technology*. New York: Noise Control Foundation, Version 94–02.
3. D. Y. Maa 1975 *Scientia Sinica* (in Chinese) **18**, 55–71. Theory and design of microperforated panel sound-absorption constructions.
4. D. Y. Maa 1987 *Noise Control Engineering Journal* **29**, 77–84. Microperforated-panel wideband absorbers.
5. J. Kang and H. V. Fuchs 1997 *Proceedings of the* 31*st International Acoustical Conference* (*IAC*)—*European Acoustics Association* (*EAA*) *Symposium*, *Zvolen*, *Slovakia*, 68–69. The absorption of open weave textiles and micro-perforated membranes backed by an air space.
6. Institute of Building Physics 1983 *Internal report of Tsinghua University* (in Chinese), *Beijing*. Sound absorption measurements of micro-aperture glass-fibre textiles.
7. J. Kang, X. Zha and H. V. Fuchs 1998 *Proceedings of the* 16*th International Congress on Acoustics*, *Seattle*, *Washington*, 2743–2744. Sound absorbers using microperforated layers.
8. Lord Rayleigh 1987 *Theory of Sound* (two volumes). New York: Dover; second edition, 1945 re-issue.
9. I. B. Crandall 1926 *Theory of Vibrating Systems and Sound*. New York: Van Nostrand.
10. W. T. Chu 1986 *Journal of the Acoustical Society of America* **80**, 555–560. Transfer function technique for impedance and absorption measurements in an impedance tube using a single microphone.
11. J. Krüger and M. Quickert 1997 *Applied Acoustics* **50**, 79–89. Determination of acoustic absorber parameters in impedance tubes.
12. J. Kang 1993 *Internal Report of Fraunhofer-Institut für Bauphysik*, *Stuttgart*. Mehrschichtige Folien Absorber.